Journal Pre-proof

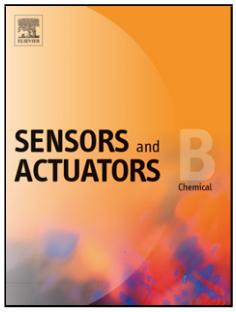

Novel rhodamine based chemosensor for detection of Hg^{2+}: Nanomolar detection, real water sample analysis, and intracellular cell imaging

Balasaheb D. Vanjare, Prasad G. Mahajan, Hyang-Im Ryoo, Nilam C. Dige, Nam Gyu Choi, Yohan Han, Song Ja Kim, Chong-Hyeak Kim, Ki Hwan Lee

PII: S0925-4005(20)31648-8

DOI: https://doi.org/10.1016/j.snb.2020.129308

Reference: SNB 129308

To appear in: *Sensors and Actuators: B. Chemical*

Received Date: 17 August 2020

Revised Date: 28 November 2020

Accepted Date: 1 December 2020

Please cite this article as: Vanjare BD, Mahajan PG, Ryoo H-Im, Dige NC, Choi NG, Han Y, Kim SJ, Kim C-Hyeak, Lee KH, Novel rhodamine based chemosensor for detection of Hg^{2+}: Nanomolar detection, real water sample analysis, and intracellular cell imaging, *Sensors and Actuators: B. Chemical* (2020), doi: https://doi.org/10.1016/j.snb.2020.129308

Novel rhodamine based chemosensor for detection of Hg^{2+}: Nanomolar detection, real water sample analysis, and intracellular cell imaging

Balasaheb D. Vanjare[1], Prasad G. Mahajan[1], Hyang-Im Ryoo[1], Nilam C. Dige[2], Nam Gyu Choi[1], Yohan Han[2], Song Ja Kim[2], Chong-Hyeak Kim[3], Ki Hwan Lee*[1]

[1]Department of Chemistry, Kongju National University, Gongju, Chungnam 32588, Republic of Korea.

[2]Department of Biological Science, Kongju National University, Gongju, Chungnam 32588, Republic of Korea.

[3]Center of Chemical Analysis, Korea Research Institute of Chemical Technology, Yuseong Daejeon 34114, Republic of Korea.

Corresponding author: khlee@kongju.ac.kr (Ki Hwan Lee)

Graphical Abstract

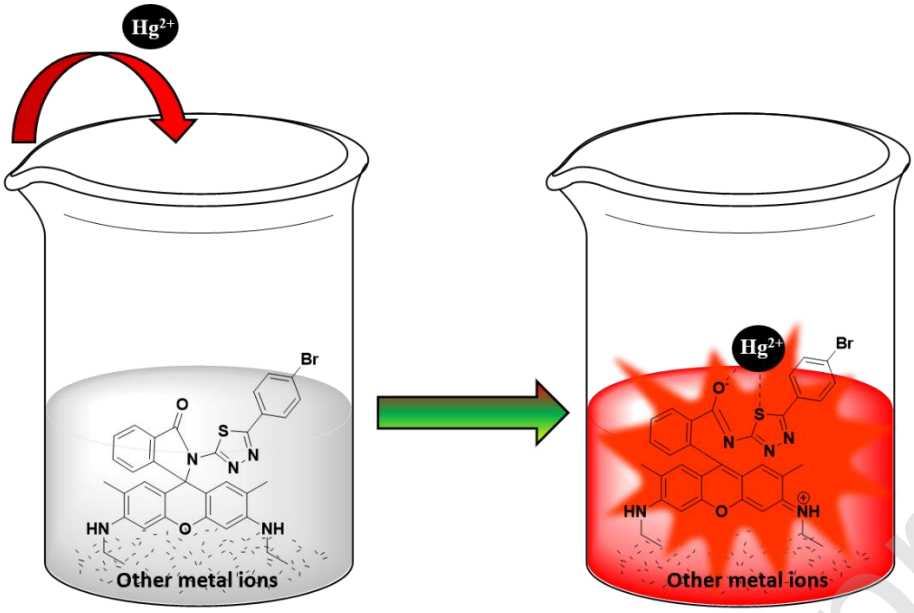

Highlights:

- Novel Rhodamine 6G based chemosensor **PS** was designed and synthesized.
- The proposed chemosensor **PS** exhibit high selectivity and sensitivity towards Hg^{2+} metal ion.
- Detection limit for Hg^{2+} metal ion could be measured at nano molar (30.37 nM) level.
- The stoichiometry between probe PS and Hg^{2+} ion was found to 1:1.
- The probe **PS** can successfully use for sensing Hg^{2+} ions in aqueous media and living cells (MDA-MB-231 & A375).

Abstract

A novel fluorescent chemosensor **PS** founded on rhodamine 6G for Hg^{2+} has been synthesized and authenticated by employing ^{1}H NMR, ^{13}C NMR, and LC-MS skills. The fluorescent chemosensor displays an intense selectivity and sensitivity for Hg^{2+} over additional metal ions explored in the combined organic aqueous phase. A strong fluorescence enhancement was

detected after the addition of Hg^{2+}, which was accompanied by ring-opening of a rhodamine spiro-cyclic structure. The stoichiometric ratio of the PS-Hg^{2+} complexes was determined to be 1:1 according to Job's plot and ^{1}H NMR experiment. The binding constant and detection limit (LOD) for PS-Hg^{2+} complexation is estimated to be 6×10^{4} M^{-1} and 3.0375×10^{-8} M (30 nM), respectively. The extreme fluorescent enhancement caused by Hg^{2+} binding in chemosensor PS occurred at a pH range of 6-8. Owing to practical application, the Hg^{2+} metal ion was efficiently determined using a spike and recovery approach from real water samples. Additionally, the probe PS was further used in the cell imaging experiment for the detection of the Hg^{2+} intracellularly using MDA-MB231 and A375 breast cancer cells by MTT assay method with low cytotoxicity.

Keywords

Rhodamine derivative; Chemosensor for Hg^{2+} detection; Nano molar detection; Cell imaging; cytotoxicity.

1. Introduction

The design of optical chemosensors for selective appreciation and sensing anticipated metal ions is an essential and modern research field. In this regard, the metal selective fluorescent

chemosensors function as a valuable tool for identifying the distinct metal ions. Therefore, the fluorescent chemosensors have been widely utilized to detect biologically and environmentally related metal ions[1–4]. There are several metal ions that exist on earth. Among them, some are toxic, and others are nontoxic to the living organism. Mercury is one of the highly vital heavy transition metal ions (HTM), which is considered as one of the most dominant toxic metal elements in the environment. And three types of mercury exist: the types are an element, an inorganic species, and an organic species [5–7]. Among all, organic species is one of the utmost toxics, by means of both naturally as well as artificially. It can effortlessly pass through the biological membrane such as skin, breathing, and gastrointestinal tissues [8–10]. It has been substantiated that, mercury ion can cause a broad range of disorders such as serious cognitive, motion disorders, and brain damage. Therefore, it is extremely imperative to develop a new system which can easily detect the metal ions which is harmful to the living organism or environment. At present, chemosensor is one of the most effective approaches which has been extensively utilized for the detection of various analytes. Hence, a great deal of attention has been devoted to creating successful chemosensor to track the trace quantity of harmful metal ions. [11–14].

However, up to date detecting heavy metal ions for environmentally and clinical samples are mainly based upon atomic absorption/ emission spectroscopy, inductively coupled plasma mass spectroscopy (ICP-MS), capillary electrophoresis, and high-performance liquid chromatography. However, the wide utilization of these methods is largely limited because these techniques demand the expensive and complicated sample pretreatment and instrumentation [15–17]. Owing to the features of high sensitivity, selectivity, and less expensive cost, the fluorescent chemosensors have attracted significant devotion and progressively becomes a crucial research area for sensing of heavy metal ions or anions [18–20, 60, 61]. Recently, rhodamine and its derivatives have received increasing attention in the design of chemosensors for metal ion detection. Rhodamine derivatives recognized for good solubility, high quantum yield, long excitation wavelength, and large molar absorption coefficient. Under these fascinating properties, various rhodamine based chemosensors have been widely used for the recognition of the numerous analytes. The metal ion sensing mechanism of these sensors is based on the change in the structure between the spirocyclic and open-cycle forms [21–24]. Furthermore, rhodamine based chemosensors can accomplish fluorescence turning on/off together with an obvious color

change from colorless to pink. Thus, most of the chemosensors comprise of rhodamine core structure, especially for Hg^{2+} metal ion based sensors are of chromogenic and fluorogenic types [25a].

Herein, we report our work in the design and synthesis of rhodamine based organic compound that is 2-(5-(4-bromophenyl)-1,3,4-thiadiazol-2-yl)-3',6'-bis(ethylamino)-2',7'-dimethylspiro [isoindoline-1,9'-xanthen]-3-one **(PS)** that selectively detects Hg^{2+} metal ion. Agreeably, the synthesized novel chemosensor PS demonstrates extremely selective and sensitive fluorescent enhancement after the addition of the Hg^{2+} because of the chelation enhanced fluorescence phenomenon. As per the practical application point of view, the present method was successfully applied for the quantitative determination Hg^{2+} metal ion by using real water samples (tap and drinking water) and also utilized for the intracellular bio-imaging of the mercury (II) ion using two cells i.e. A375 and MDA-MB-231.

2. Experimental Section

2.1 Materials and instrumentations

Rhodamine 6G, Thiosemicarbazide, 4-bromo benzoic acid, and potassium tert-butoxide were purchased from Sigma Aldrich. Tetrahydrofuran (THF), ethyl acetate (EtOAc), dichloromethane, and methanol were procured from a commercial vendor (Samchun chemicals Korea). All the chemicals were used without purification. Shimadzu Spectrophotometer (Scinco, Korea) was used for absorption spectra and FS-2 fluorescence spectrometer (Scinco, Korea) was used for the fluorescence study. For all the samples, the absorption and fluorescence analysis done at room temperature. In a fluorescence study, the samples were excited at 530 nm. The LC-MS has inspected on 2795/ZQ2000 (waters) spectrometer. FT-IR spectra were recorded on a Frontier IR (Perkin Elmer) spectrometer using KBr pellets. ^{1}H NMR and ^{13}C NMR spectra were recorded on Bruker Avance 400 MHz spectrophotometer (400 and 100 MHz for proton and carbon NMR) in which TMS is used as an internal standard. The melting point measured by using the MPA 160 instrument of Fisher Scientific (USA). In the existence and non-existence of the Hg^{2+}, the fluorescence time decay performance of the probe PS was measured at respective wavelength by a time-correlated single-photon counting (TCSPC) spectrophotometer (HORIBA-Ihr320, Japan). As a result, obtained outputs were examined on data station software provided with an

instrument for the assessment of fluorescence lifetime values of probe PS in the presence and absence of the Hg^{2+}.

2.2 Preparation of the metal ions solution for optical studies

A stock solution of probe **PS** (1 mM) was prepared in tetrahydrofuran (THF) solvent and the stock solution of all the metal ion (1 mM) containing Hg^{2+}, Ba^{2+}, Ca^{2+}, Cd^{2+}, Co^{2+}, Cu^{2+}, Fe^{2+}, Mg^{2+}, Mn^{2+}, Ni^{2+}, Pb^{2+}, Zn^{2+}, Al^{3+}, Cr^{3+}, Fe^{3+}, Na^{+}, K^{+}, Cu^{+} and Ca^{+}, etc. were prepared by dissolving corresponding salts in double-distilled water. Earlier to spectroscopic measurement, the known amount of stock solution of probe PS was added to a 10 ml volumetric flask followed by addition of known volume of corresponding metal ion and pH 7 solution, and finally diluted to the equivalent concentrations by using THF : water (8:2, v/v) system [25b]. Afterword, the absorption, and fluorescence intensity were recorded after 10 minutes for all the samples. For fluorescence measurement, all the samples were excited at 530 nm. The excitation and emission slits were both set for 5 nm [21].

2.3 Synthesis

*2.3.1 Synthesis of 5-(4-bromophenyl)-1,3,4-thiadiazol-2-amine (**1A**)*

The intermediary **1A** was synthesized by following the formerly published article [26]. To a 100 round bottom flask (RBF) was added 4-Bromo-Benzoic acid (0.5 gm, 2.4 mmol) and thiosemicarbazide (0.24 gm, 2.73 mmol) in $POCl_3$ (3 mL). The reaction mixture was heated to 75-80°C. After 1 hour, stopped the heating and the reaction mass gradually cooled to room temperature. Further, the reaction mass was cooled to 0-5°C and slowly quenched with distilled water and again the reaction mass was refluxed for 5 hours. Afterward, the reaction mixture was gradually cooled to ambient temperature followed by cooling to 0-5°C and basified (pH=8) with 50% NaOH. The suspended solid material stirred for an additional 1 hour at 0-5°C then filtered, dried, and recrystallized in absolute ethanol to afford a compound **1A**, which was further used for the next step.

*2.3.2 Synthesis of 2-(5-(4-bromophenyl)-1,3,4-thiadiazol-2-yl)-3',6'-bis(ethylamino)-2',7'-dimethylspiro[isoindoline-1,9'-xanthen]-3-one **(PS)***

To a mixture of rhodamine 6G (0.5 gm, 1.042 mmol), 2-Amino-5-{4-bromophenyl}-1, 3, 4-thiadiazole (0.32 gm, 1.042 mmol) in ethanol (5 ml) at ambient temperature under nitrogen atmosphere. The reaction mixture was stirred for 10 min at ambient temperature then slowly

added potassium tert-butoxide (0.14 gm, 1.252 mmol) and continued the reaction until the completion of the reaction (12 h) under nitrogen atmosphere [24]. After completion of the reaction (monitored by TLC), the reaction mixture was quenched with cold water (15 mL) and extracted with ethyl acetate (3 x 15 mL). The ethyl acetate layer was washed with water (10 mL) followed by brine solution (15 mL). The organic layer was dried over anhydrous sodium sulphate and distilled under vacuum and purified by column chromatography using (dichloromethane/methanol) as an eluent to afford a pink Solid, Yield: 85%, M.P: > 260°C; **Fig. S1:** ^{1}H NMR (DMSO-d_6, 400 MHz) δ (ppm): δ 8.58 – 6.78 (m, 8H), 6.25 (m, 4H), 5.76 (s, 2H), 3.19 – 3.09 (q, 4H), 1.82 (s, 6H), 1.20 (t, 6H). **Fig. S2:** ^{13}C NMR (101 MHz, DMSO) δ 167.25, 147.77, 135.44, 132.63, 132.22, 131.52, 129.22, 128.90, 104.44, 37.39, 14.20. **Fig. S3:** IR (KBr) ν/cm^{-1}: 3022.19, 2889.70, 2299.44, 1946.44, 1693.56, 967.13, 903.90. **Fig. S4:** LC-MS: 654.4 m/z. (M+2) **Fig. S5:** GCMS: 653 m/z.

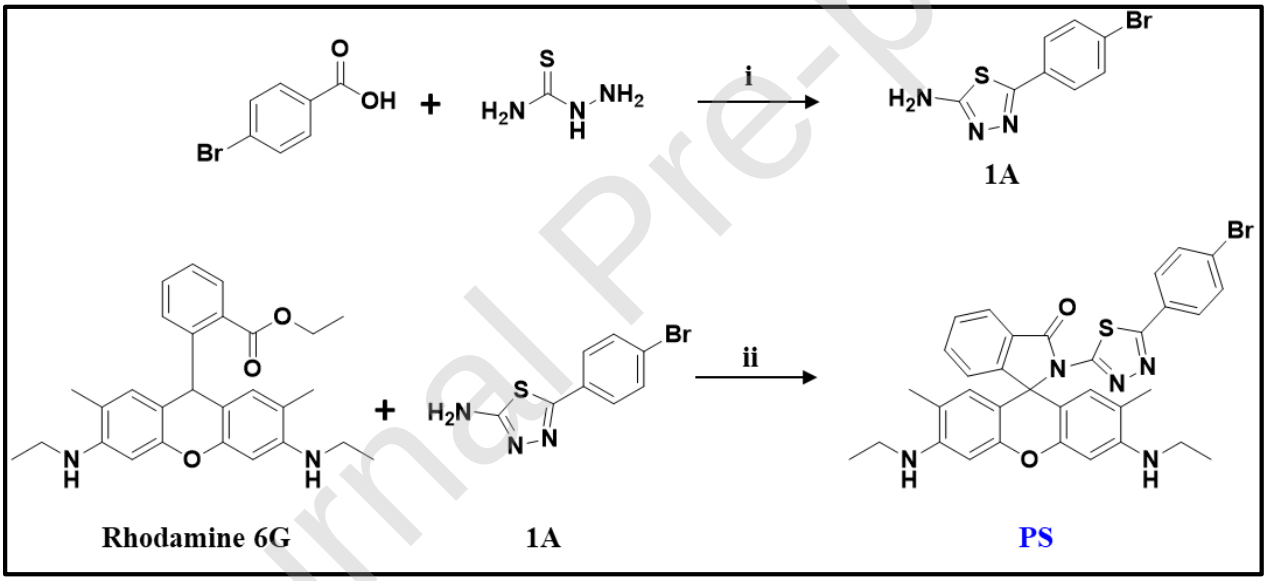

Scheme 1: Synthesis route, reagents, and conditions: i) $POCl_3$, Reflux 1 hr.; H_2O and reflux 5 hr. ii) Potassium tert-butoxide, ethanol, RT, 12 hr. Potassium tert- butoxide.

2.4 Cell imaging study

2.4.1 Cell culture and treatment

The human melanoma cancer cell line A375 and breast cancer cell line MDA-MB-231 used in this study were obtained from the KCLB (Korean Cell Line Bank, Seoul, Korea). A375 cells were cultured in Dulbecco's modified Eagle's medium (DMEM; Gibco; Thermo Fisher

Scientific, Inc., Waltham, MA, USA) and MDA-MB-231 cells were cultured in RPMI-1640 (Gibco; Thermo Fisher Scientific, Inc., Waltham, MA, USA). Both media containing 10% heat-inactivated fetal bovine serum (FBS; Tissue Culture Biologicals. Long Beach, CA, USA), streptomycin (50 µg/mL; Sigma-Aldrich, Merck KGaA, Darmstadt, Germany), and penicillin (50 unit/mL; Sigma-Aldrich). These cells were grown at 37°C in a humidified incubator with 5% CO_2. Probe (10 µM) was dissolved in dimethyl sulfoxide (DMSO; Sigma-Aldrich) and solutions of Hg^{2+} was prepared in distilled water. In this experiment, the already grown cell (MDA-MB-231 and A375) were untreated (Control) or treated with probe PS (10 µM) in the growth medium for 3 h followed by two times washing with PBS. Later, the cells were then incubated with different concentrations of Hg^{2+} (5 and 10 µM) for 3 h and then it was washed two times with PBS at 37°C. The images of both the cells were achieved using a fluorescence microscope [30].

2.4.2 Cell viability assay

The consequence of probe PS and complex of PS-Hg^{2+} on cell viability was strongminded by MTT (3-(4,5-dimethylthiazol-2-yl)-2-5 diphenyl tetrazolium bromide) assay. A375 melanoma and MDA-MB-231 cells were seeded at the density of 0.4×10^5 and 0.2×10^5 cells respectively in each well of 96-well plate. Cells were treated with probe PS at 10 µM, 10 µM of Hg^{2+} and co-treated with varying concentrations of probe (5 and 10 µM) for 24 hrs. Inhibition of cell viability was scrutinized by MTT assay (10 µl MTT/100 µl cells), as described previously [27], The optical absorbance was measured at 570 nm by using a microplate reader.

2.4.3 In-Vitro Fluorescence Imaging Study

The fluorescence intensity of A375 and MDA-MB-231 cells were confirmed by a fluorescence microscope (BX51, Olympus, Tokyo, Japan), as described previously [28]. Briefly, MDA-MB-231 and A375 cells were seeded at 1.5 x10^5 cells in a 35 mm culture plate. Further, cells were examined under green light (wavelength was 532 nm).

3. Results and Discussion

3.1. Effect of pH

To verify the output of the probe **PS** in contrast to different pH ranges have been demonstrated using the UV-Visible absorption experiment. In which the distinct pH solution prepared to vary from pH 3 to 10 and used to strengthen the best operating range for the current chemosensor **PS**.

From the pH titration experiment, it has been found that metal-free chemosensor PS exhibit low absorbance values, at pH 8-10. Whereas the absorbance values increase towards low pH because the protonation induced ring-opening phenomenon. However, after mixing the Hg^{2+} metal to the chemosensor PS the absorbance was higher at a pH range 6-8, afterwards the absorbance rates decline promptly in a highly basic condition i.e. pH 9-10 as revealed in Fig.1. The low absorbance values obtained at high pH values, which suggest that the Hg^{2+} metal ion may get hydrolyzed into its hydroxide form and that could not form a complex with the chemosensor PS. Therefore, from the above experiment, we have opted to retain the pH=7.0 in the entire experiment and the same system is suitable for the cell biology experiment as well.

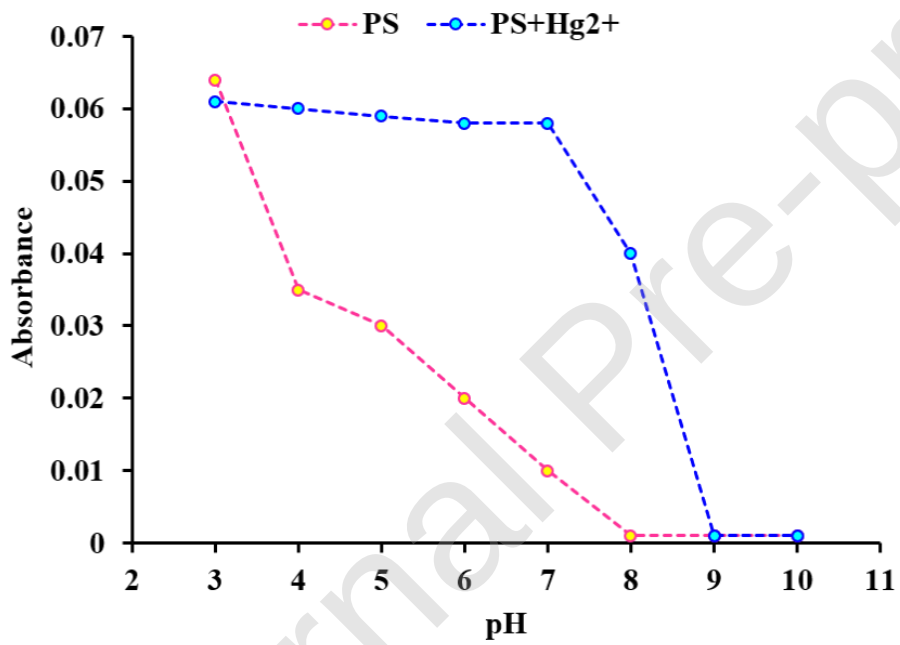

Fig. 1. Effect of pH on absorbance of chemosensor PS (10 µM) in absence and presence of Hg^{2+} (50 µM)

3.2 Spectroscopic properties

3.2.1 Selectivity of probe PS using absorption and fluorescence studies

To explore the sensing assets and its sensitivity of the probe **PS** against various metal ion viz. Ba^{2+}, Ca^{2+}, Cd^{2+}, Co^{2+}, Cu^{2+}, Fe^{2+}, Mg^{2+}, Mn^{2+}, Ni^{2+}, Pb^{2+}, Zn^{2+}, Al^{3+}, Cr^{3+}, Fe^{3+}, Na^{+}, K^{+}, Cu^{+} and Ca^{+}, etc. can be identified by using UV-Vis absorbance and fluorescence study in THF: water system (8:2, v/v, at pH=7.0). In UV-Vis absorption experiment, the absorption spectra of

the probe **PS** (10 µM) in a mixed organic and aqueous system does not show up any response beyond 500 nm (**Fig. 2A**), which demonstrates that the probe PS exists in the closed spirocyclic form (non-fluorescent) rather than open ring (fluorescent) in mixed organic and aqueous solvent phase [29]. Furthermore, there were no more substantial variations noticed due to the addition of 5.0 equivalents of the various metal ions (such as alkali, alkaline earth group, transition, and non-transition metal) except for Hg^{2+}. But, after the addition of the Hg^{2+}, a great transformation was observed in the absorption spectrum which indicates that probe PS can selectively discriminate the Hg^{2+} metal ion.

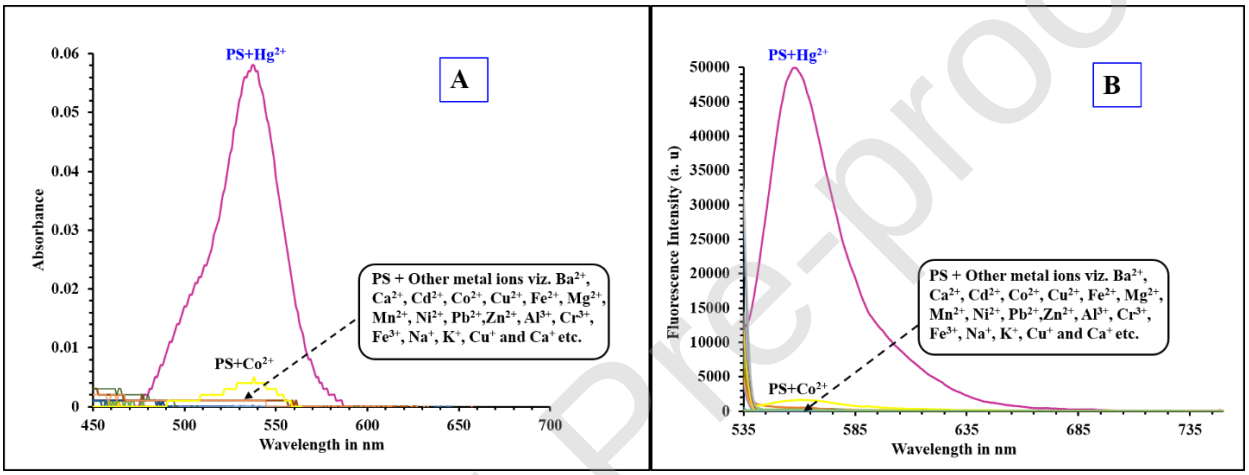

Fig. 2. (A) Absorption spectrum of the probe PS (10 µM) in presence of various metal ions. (B) Fluorescence emission spectrum of the probe PS (10 µM) in presence of various metal ions.

Likewise, the selectivity of the probe **PS** for Hg^{2+} metal ion further principally inspected by using fluorescence spectroscopy technique in the mixed organic and aqueous system (THF: Water, 8:2, V/V, pH=7). As displayed in **Fig. 2B**, probe PS is non-fluorescent because of its closed five-membered spirolactam framework. When probe PS was integrated with a series of the numerous metal salts (5.0 equiv.) viz. Ba^{2+}, Ca^{2+}, Cd^{2+}, Co^{2+}, Cu^{2+}, Fe^{2+}, Mg^{2+}, Mn^{2+}, Ni^{2+}, Pb^{2+}, Zn^{2+}, Al^{3+}, Cr^{3+}, Fe^{3+}, Na^{+}, K^{+}, Cu^{+} and Ca^{+}, etc., it does not create any substantial variation in an emission spectra. But, after integrating the probe PS with Hg^{2+} metal ion a sensational shift as well as marvelous fluorescent enhancement was noticed in the emission spectra at 558 nm; which makes the probe PS as a "turn on" fluorescent chemosensor for the detection of the Hg^{2+} metal ion (**Fig. 2B**). A noticeable variation was observed in case of Hg^{2+} metal ion which

reinforces that, probe PS after interaction with Hg^{2+} exist in the Spirolactam open ring form (fluorescent).

3.2.2 Effect of the PS-Hg^{2+} over other metal ions

In chemosensor development, achieving the selectivity and sensitivity across other metal ions is a demanding and obligatory task. Therefore, to explore the consequence of the other co-existing metal ions on the emission intensity, we have conducted the competing metal ion experiment. To investigate the impact of the participating metal ions on the fluorescence intensity of probe PS (10 µM) induced by Hg^{2+} (50 µM), other metal ion-containing Ba^{2+}, Ca^{2+}, Cd^{2+}, Co^{2+}, Cu^{2+}, Fe^{2+}, Mg^{2+}, Mn^{2+}, Ni^{2+}, Pb^{2+}, Zn^{2+}, Al^{3+}, Cr^{3+}, Fe^{3+}, Na^{+}, K^{+}, Cu^{+} and Ca^{+} (50 µM) was incorporated to the solution holding a combination of **PS** and Hg^{2+} in a mixed organic and aqueous system. The fluorescence emission intensity outcomes of the probe **PS** in presence of each metal ions (red pillars) and probe PS+ Hg^{2+} ion in the presence of the other metal ions (green pillars) have been shown in **Fig 3.** The examined background metal ions displayed a slight or no interference with the recognition of the Hg^{2+} metal ion. Besides, as presented in Fig. 3 (red pillars), the Co^{2+} metal ion exhibits slightly more response in fluorescence emission intensity as compared with the other metal ions over PS-Hg^{2+} complex. However, the fluorescence intensity of the Ps-Hg^{2+} complex was not significantly affected even if the Co^{2+} metal ion presence in the same solution. Remarkably, the study of the foreign metal ions could not interfere and influence on the detection of the Hg^{2+} metal ion by the addition of the various analytes. Thus, the obtained results imply that fluorescence intensity response in the direction of studied metal ions exhibits selectivity and sensitivity for Hg^{2+} metal ion.

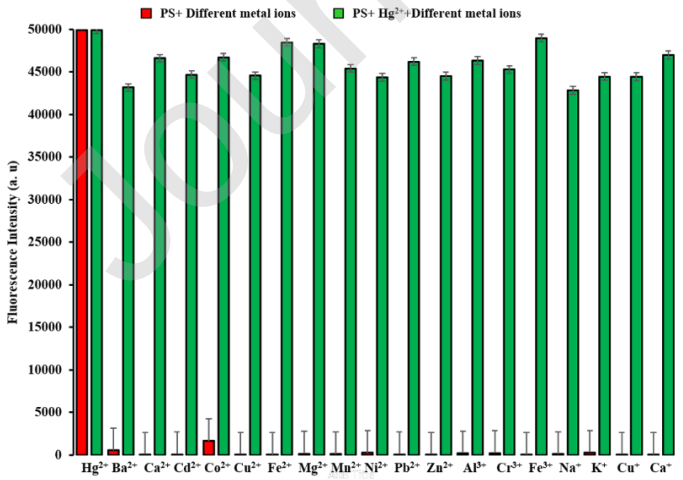

Fig. 3. The selectivity and competition of probe PS (10 µM) for Hg^{2+}(50 µM). The pillars in the front row represent the fluorescence response of probe PS (10 µM) for the examined metal ions. The back pillars represent the successive addition of Hg^{2+} (50 µM) to the solution including PS (10 µM) and the other metal ions (50 µM), respectively (λ_{ex} =530 nm).

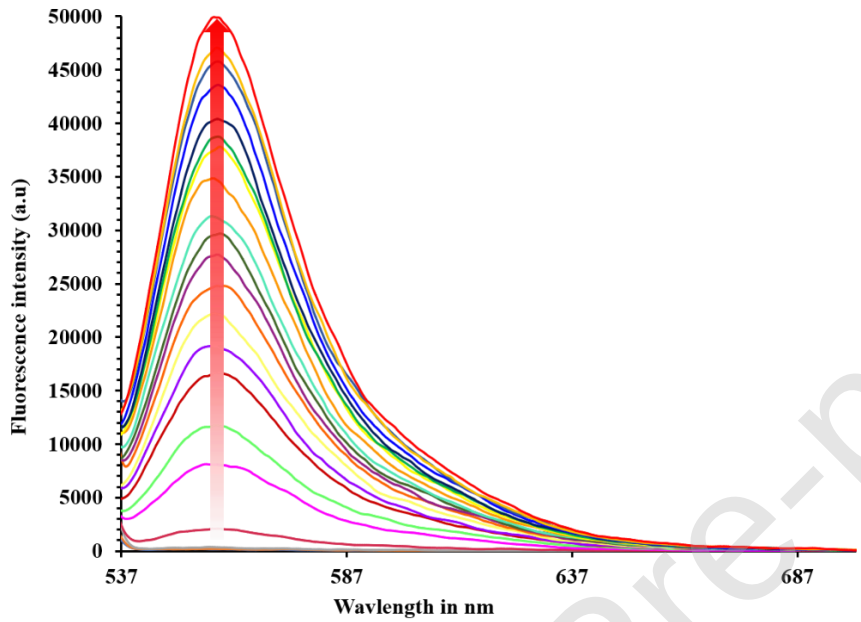

Fig. 4. Fluorescent intensity (λ_{ex}=530 nm) changes of PS (10 µM) in THF: Water (v/v; 8:2; pH=7) upon the incremental addition of the Hg^{2+} ion (0-10 µM).

3.3 Statistical Data Analysis

3.3.1 Fluorescence titration and limit of the detection (LOD)

The fluorescence intensity of the probe **PS** in the existence and non-existence with Hg^{2+} metal ion within the concentration range of 0-10 µM was thoroughly presented in **Fig. 4**. It has been found that the fluorescence emission strength of the probe **PS** surges linearly with the incremental addition of the Hg^{2+} metal ion within the range between 0-10 µM. From the above result, a graph of fluorescence intensity against [Hg^{2+}] was plotted which obeys a straight-line equation shown in **Fig. 5**. The straight-line equation is well fitted to the fluorescent incremental enhancement results in a range of 0-10 µM. The limit of the detection (LOD) was computed [30–32] by utilizing equation 1 and is observed to be 3.0375 × 10^{-8} M (30 nM).

$$LOD = \frac{3.3\ \sigma}{K} \qquad (1)$$

Where σ and K represent the standard deviation of the blank measurement and slope between the fluorescence intensity to the Hg^{2+} metal ion concentration. Besides, the LOD was calculated by using the current method is considerably much lower than the previously reported method. A comparison table has been prepared to compare the LOD of the present method with other reported methods concerning solvent for Hg^{2+} metal ion (**Table. 1**).

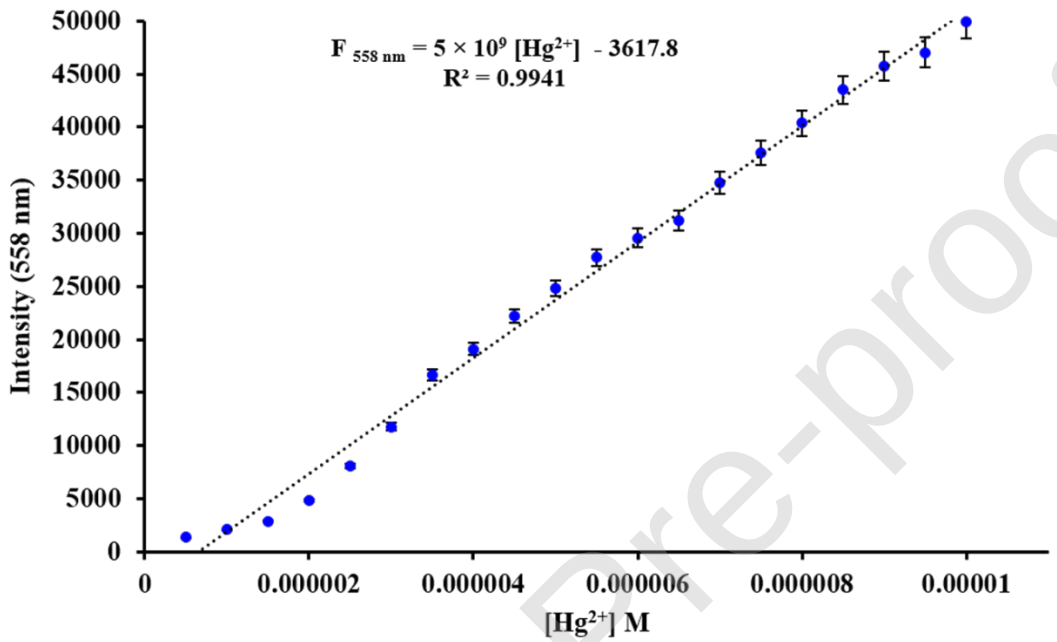

Fig. 5. A Plot of emission intensity of **PS** (10 µM) at 558 nm versus concentrations of Hg^{2+} (0-10 µM).

Table 1: Comparison syntax among reported fluorescent probes and present chemosensor **PS** with respect LOD of Hg^{2+}.

Sr. No	Detection method operated	Chemosensor used	Solvent system used	Real sample analysis	LOD	Ref. No
1	Fluorescence	Thiosemicarbazone	0.01 M acetic acid/ sodium acetate buffer	-	0.77 µM	[33]
2	Fluorescence	GT capped AgNPs	Double distilled water	Tap/River water, Catalytic activity	0.037 nM	[34]

3	Fluorescence	Azo Crown ether	Methanol	-	13.9 µM	[35]
4	Amperometry	Polyaniline-naflon nanostructure	-	-	0.05 µM	[36]
5	Potentiometric	Poly (vinyl chloride)	-	Tap water	0.02 µM	[37]
6	Spectrophotometry	Ruthenium complex	Ethanol	-	0.1 µM	[38]
7	Colorimetric	Silver nanoparticles	Aqueous solution	Tap/ Lake water	0.85 µM	[39]
8	Spectrophotometry	Rhodamine derivatives	Aqueous solution	Digital information	77 nM	[40]
9	Potentiometric	Gold nanoparticles	Doubly distilled water	Sewage water	0.05 µM	[41]
10	Colorimetric	Gold nanoparticles	Ultrapure water	Pond / River water	50 nM	[42]
11	Colorimetric	Biosynthesized AuNPs	Deionized milli-Q water	-	1.44 µM	[43]
12	Amperometry	Modified carbon paste	Citrate phosphate buffer (0.1 M, pH 7.0) with a glucose solution (12.2 mM)	Natural water	2.5 µM	[44]
13	Electrochemical	Thiol functionalized reduced GO	Milli-Q water	Tap water	0.2 µM	[45]
14	Fluorescence /Colorimetric	coumarin 3-azomethine derivative (AGB)	DMSO: Water (1:99, v/v)	Intracellular cell imaging	45 µM /22 µM	[46]

15	Fluorescence	2-Hydroxy benzothiazole modified rhodol	THF: HEPES (4:6, v/v)	Intracellular cell imaging	0.27 µM	[47]
16	Fluorescence	Double naphthalene Schiff base	DMSO	-	0.0559 µM	[48]
17	Fluorescence	Nitrogen-doped carbon quantum dots	Aqueous solution	Tap/ Lake water	0.23 µM	[49]
18	Fluorescence	copolymer of carbazole and thieno [3,4b]-pyrazine	THF	-	0.1 µM	[50]
19	Fluorescence	Amino Acid Based Sensor	Water: DMF (98:2, v/v, 10 mM HEPES)	-	57.2 nM	[51]
20	Fluorescence	Squaraine–bis(rhodamine-6G)	Acetonitrile	-	0.0169 µM	[52]
21	Fluorescence	Squaraine based fluorescent probe	Ethanol: Water (20:80, v/v)	-	0.0219 µM	[53]
22	Fluorescence	Rhodamine appended terphenyl	THF	-	0.5 µM	[54a]
23	Fluorescence	Tetraphenyl ethylene based AIE probe	Water	Intracellular cell imaging	63 nm	[54b]
24	Fluorescence	TPE–boronic acid chemodosimeter	90% Water-THF mixture		0.12 ppm	[54c]
25	Fluorescence	Rhodamine 6G based	THF: Water (8:2, v/v, pH=7)	Tap / Drinking water and Intracellular cell imaging	30.37 nM	**Present work**

3.3.2 Determination of the binding stoichiometry and binding constant complex.

To determine the binding stoichiometry between the chemosensor **PS-Hg^{2+}** complex has been studied by conducting a Jobs plot experiment [55]. In this experiment, the final sum of the mole

fraction of the ligand (**PS**) and metal (Hg^{2+}) was remained constant with simply altering the mole fraction of ligand (Hg^{2+}). **Fig. 6** signifies the Job's plot, shows the corresponding absorption values of every solution having a mole fraction 0.1-0.9 for Hg^{2+} metal ion. From this experiment, it was found that the maximum absorbance was spotted at a mole fraction around 0.5 for Hg^{2+} metal ion. Therefore, one can be concluded from the above results that, the chemosensor **PS** and the Hg^{2+} metal ions form 1:1 complex.

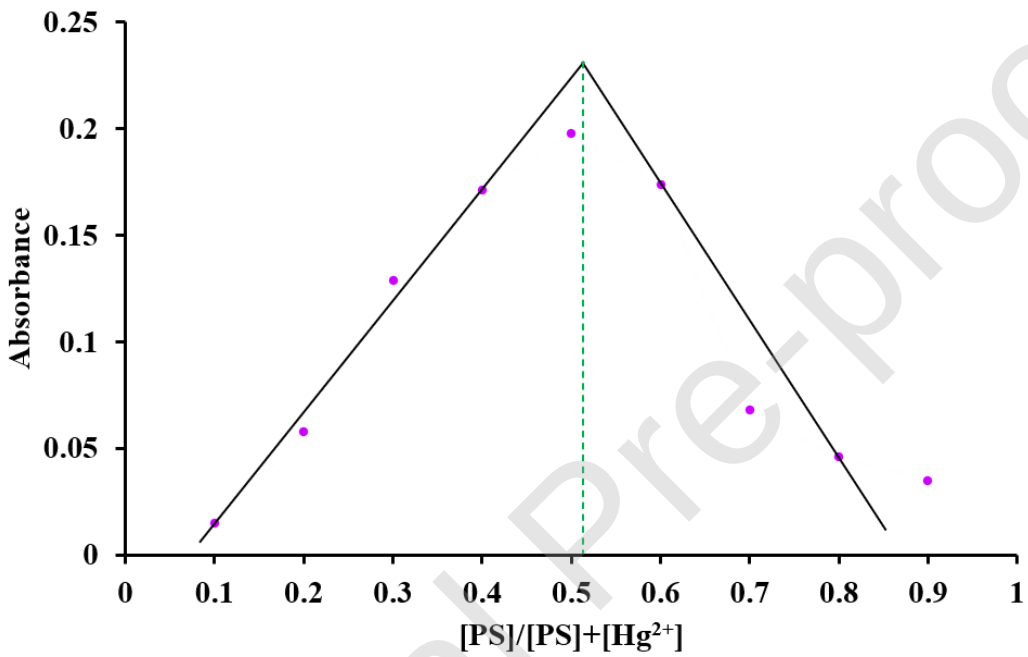

Fig. 6. Jobs plot suggesting stoichiometry among chemosensor **PS** and Hg^{2+} =1:1.

Additionally, the binding constant (K_B) between the probe **PS** and Hg^{2+} from the fluorescence intensities data (at 558 nm) by following the modified Benesi-Hildebrand equation (2) [56].

$$\frac{1}{F-F_0} = \frac{1}{F_{max}-F_0} + \frac{1}{K_B[Hg^{2+}]^n}\frac{1}{(F_{max}-F_0)} \quad (2)$$

Where, F_0, F, and F_{max} are the emission intensity (at 558 nm) of the probe **PS** in the absence of the Hg^{2+}, in the presence of Hg^{2+} at dissimilar concentration and maximum fluorescence intensity in the presence of Hg^{2+} metal ion. However, K_B is the binding constant and n is the number of Hg^{2+} metal ion bound in chemosensor **PS** and Hg^{2+} complexation (Here, *n=1*). Furthermore, the modified Benesi-Hildebrand (B-H) graph was plotted as displayed in **Fig. 7**. The obtained slope value from the linear B-H plot was used to compute the binding constant and

which demonstrate a high binding constant value, provided as $K_B = 6 \times 10^4$ M^{-1}, for 1:1 complexation developed among probe **PS** and Hg^{2+} metal ion.

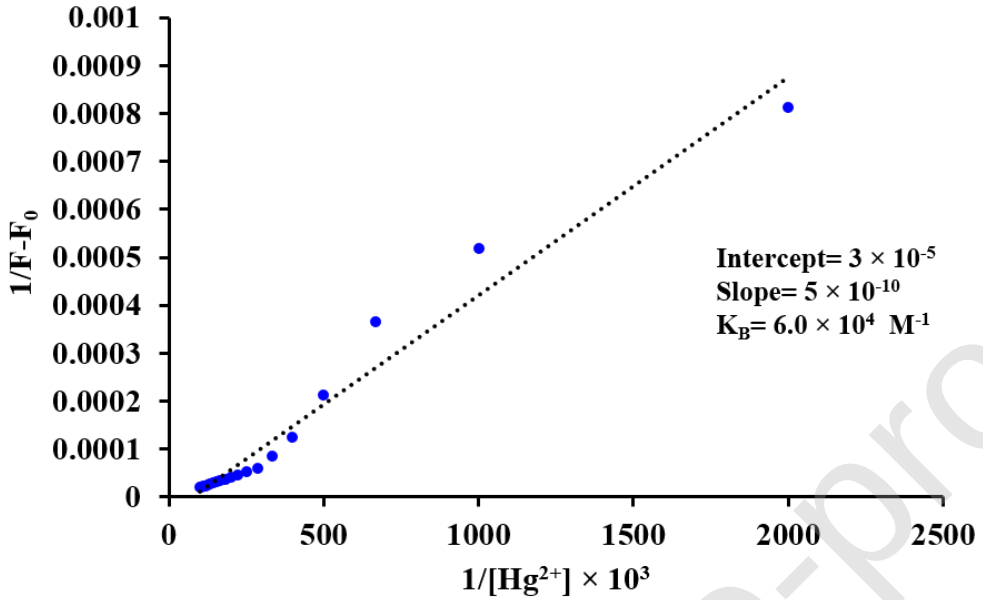

Fig. 7. Modified Benesi-Hildebrand plot of chemosensor PS-Hg^{2+} complexes in THF: Water (v/v, 8:2, pH= 7.0) solution.

3.3.3 Sensing mechanism

Rhodamine or its derivatives are an ultimate model in chemosensors study since of its unique structural property. It retains closed five-membered cyclic amide functionality (spirolactum) exhibit non-fluorescent behavior while the open-ring form of spirolactum induces a potent fluorescence emission intensity. Moreover, in the absence of heavy metal ions or cations, these probes occur in a spirocyclic form, which is colorless and non-fluorescent. But in the presence of discriminatory metal cations triggers the opening of the spirocyclic ring as a result these probes become more fluorescent or exhibiting strong fluorescence emission intensity in a fluorescence study. Therefore, it could be suggested that a spirocyclic ring-opening mechanism operates through chelation, in which the Hg^{2+} metal ion from a coordinated complex with the oxygen atom of amide functionality existing in probe **PS**. Furthermore, there are numerous reports are present on rhodamine based spirolactum chemosensors, the Hg^{2+} stimulated fluorescence enhancement of chemosensor **PS** is a highly expected outcome of the spirolactum ring-opening mechanism [47,52,54]. Thus, to scrutinize the mechanism of chelation boosted fluorescence of

probe **PS** by the addition of Hg^{2+} metal ion operated through the spirocyclic ring-opening approach. To explain in detail, we have performed several experiments including Jobs plot, ^{1}H NMR titration, and fluorescence lifetime, correspondingly.

From the Jobs plot experiment (Fig. 7), the absorbance values of titration solution demonstrate an inflection point at around 0.5, which implies the formation of the 1:1 coordination class among probe **PS** and Hg^{2+} metal ion (*i.e.* **PS-Hg^{2+}**) in a mixed organic and aqueous system (8:2, THF: Water). Likewise, the stoichiometry and coordination between probe **PS** and Hg^{2+} metal ion were confirmed by ^{1}H NMR titration experiment. In which, probe **PS** (1.0 equiv) integrated with various concentrations of Hg^{2+} metal ion such as, 0.5 and 1.0 equiv, correspondingly. **Fig 8** comprises of three distinct ^{1}H NMR spectra's (A / B & C), in which spectra A was recorded only for probe **PS** while spectra B and C comprises probe **PS** (1.0 equiv.) with 0.5 & 1.0 equivalent of Hg^{2+} respectively. As shown in **Fig 8A** and **B**, the peak was appeared having chemical shift value 5.04 ppm for N-H proton suggesting that the five-membered spirocyclic ring still present in its closed form. It means after the addition of 0.5 equivalent of Hg^{2+} metal ion-containing probe **PS** does not form a complex. However, interestingly the N-H proton gets disappeared after the addition of 1.0 equivalent of Hg^{2+} which is shown in **Fig. 8C** [57]. Therefore, the ^{1}H NMR titration experiment confirms the ring-opening mechanism initiated via a chelation approach in which metal ion binds with probe **PS** to form a complex (**PS-Hg^{2+}).** The plausible binding mode of probe **PS** with Hg^{2+} metal ion representation is shown in **Scheme 2**.

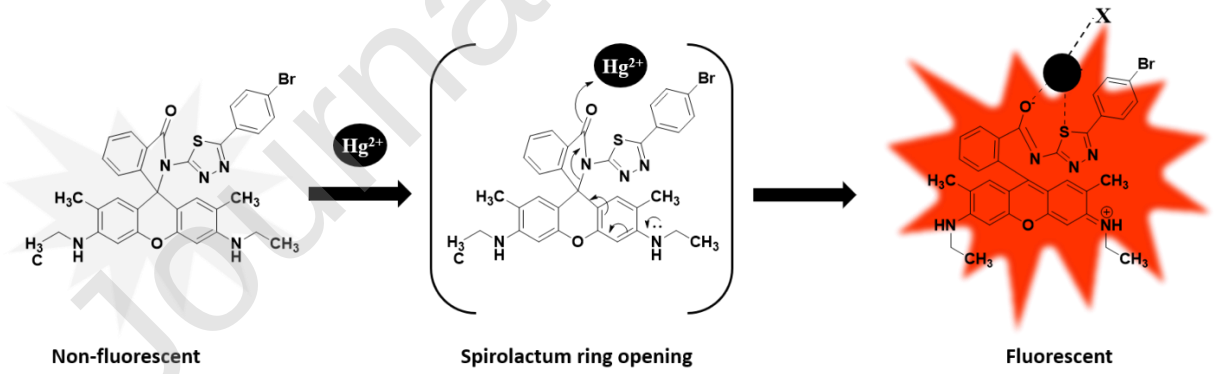

Scheme. 2. Proposed binding mode of probe **PS** with Hg^{2+} metal ion (X= coordinating anion or solvent).

Besides, the excited state complexation of probe **PS-Hg^{2+}** was further authenticated by inspecting the fluorescence lifetime values in the presence and absence of distinct concentration

of Hg^{2+} metal ion to the probe **PS** in mixed THF: water (V/V, 8:2, pH= 7) system as demonstrated in **Table 2**. Primarily, fluorescence lifetime was calculated for probe **PS**, detected to be 1.63 ns. Later, after the addition of the Hg^{2+} metal ion within the concentration scale of 0-10 µM. It was found that the fluorescent lifetime value incessantly increases with the addition of the Hg^{2+} metal ions and is found to 3.13, 3.53, and 3.91, respectively. This result indicates that enhancement of fluorescence intensity and resultant excited singlet state lifetime is noticeable through complexation owing to freezing of non-radiative pathways produced by inflexible composition of the probe **PS-Hg^{2+}** complex than the relatively more flexible composition of the probe **PS.**

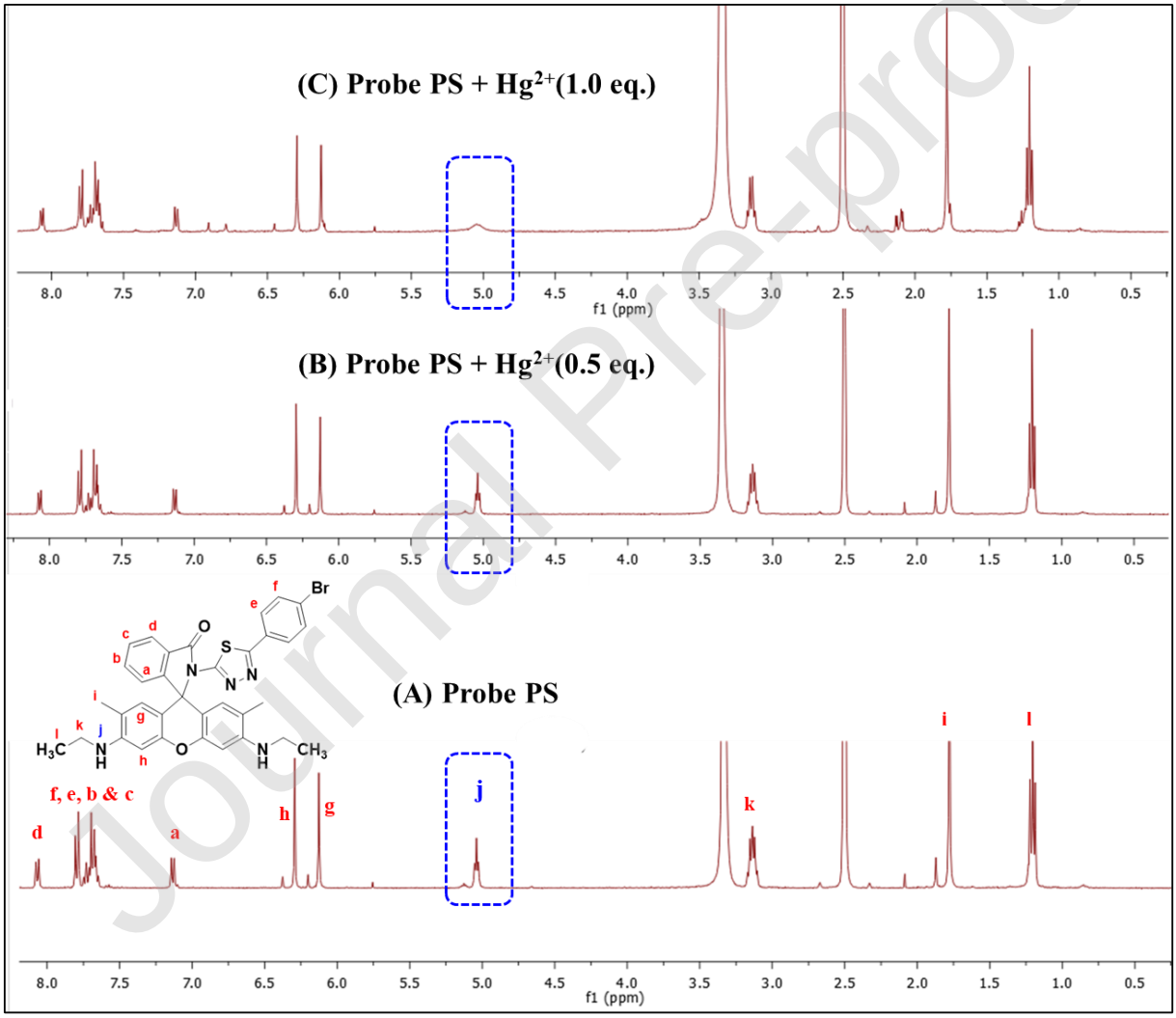

Fig. 8. ^{1}H NMR spectra of (A) 1.0 equiv. of Chemosensor PS in DMSO-d_6 (B) Chemosensor PS + 0.5 equiv. of Hg^{2+} in DMSO-d_6 (C) Chemosensor PS + 1.0 equiv. of Hg^{2+}. (*equiv. = equivalent)

Table 2: Fluorescence lifetime of probe **PS** and **PS-Hg^{2+}** complex in THF: Water (8:2) system.

Sr. No	**Concentration of added Hg^{2+} metal ion (µM)**	**Fluorescence lifetime value of** PS+Hg^{2+} **(ns)**
1	0	1.98
2	0.3	3.13
3	0.6	3.53
4	1.0	3.91

3.4. Applications of proposed fluorescence method.

3.4.1. Quantitative determination of Hg^{2+} in environmental samples using chemosensor **PS.**

The practical applicability of the invented chemosensor **PS** was assessed by using a spike and recovery approach [55]. In which the contamination of the Hg^{2+} was revealed in drinking and tap water. The samples were collected from the local campus of a university. To carry out this experiment, three distinct concentration solutions of Hg^{2+} metal ion was prepared by spiking standard solution of Hg^{2+} metal ion. The testing was performed by spiking the known amount of standard Hg^{2+} metal ion solutions. The fluorescence emission intensity of these three testers was evaluated and correlated with fluorescence emission intensity within the range of 0-10 µM which is presented in **Fig. 4**. The real water sample analysis data represented in **Table 3**. For the real water sample analysis, the calculated recovery for the known amount of Hg^{2+} added was between 96 to 100%. Hence, it reveals that the current approach can be applied for real water sample assessment.

Table 3: Determination of Hg^{2+} ion in real water samples.

Water samples studied	Amount of standard Hg^{2+} ion added (M)	Total Hg^{2+} ion found (M) (n=3)	Recovery of Hg^{2+} ions added (%)
Tap Water	0.50×10^{-6}	0.48×10^{-6}	96.00
	4.50×10^{-6}	4.45×10^{-6}	98.88

	9.50×10^{-6}	9.47×10^{-6}	99.68
Drinking Water	0.50×10^{-6}	0.49×10^{-6}	98.00
	4.50×10^{-6}	4.49×10^{-6}	99.77
	9.50×10^{-6}	9.49×10^{-6}	99.89

3.4.2 Intracellular cell imaging of Hg^{2+} utilizing chemosensor (**PS**) and cytotoxicity studies:

3.4.2.1 Cell imaging

Mercury is a naturally occurring element found in air, soil, and water. Mercury is one of the most dangerous among the top ten chemicals as per WHO. The inhalation of mercury can cause severe health issues on human health such as effects on the nervous, immune, digestive system, kidneys, and lungs problem, and chances of fatal [58,59]. Therefore, to overcome this concern, we have synthesized and developed such a chemosensor that possesses a high rate of selectivity as well as sensitivity towards Hg^{2+} metal ion. To verify the reliability and functional capability of the present chemosensor, we have conducted a bioimaging study [27,30]. In which the synthesized chemosensor **PS** with or without treating with Hg^{2+} were explored on two cancer cell lines specifically MDA-MB-231 and A375, respectively. In this experiment, the cultured cells were systemically treated with probe PS, Hg^{2+} metal ion at various concentrations and the fluorescence images acquired for the various models have been displayed in **Fig. 9 & 10**. The fluorescence images exhibited in **Fig. 9** comprise, probe **PS** (10 μM) in DMSO (B1), **PS** (10 μM) + 5 μM of Hg^{2+} (B2), and **PS** (10 μM) + 10 μM of Hg^{2+} (B3) for MDA-MB-231 cell. Likewise, **Fig. 10** encompasses, probe **PS** (10 μM) in DMSO (M1), **PS** (10 μM) + 5 μM of Hg^{2+} (M2), and **PS** (10 μM) + 10 μM of Hg^{2+} (M3), respectively. Fluorescence microscopy measurements at an excitation wavelength (green light) of 532 nm were used to assess the fluorescence images. The fluorescence and bright-field transmission images of test samples were equated with control for living MDA-MB-231 and A375 cell as shown in **Fig. 9 & 10.** The experimental results indicate that both the figures exhibit high fluorescence when the probe **PS** and Hg^{2+} metal ion are interacting with each other. In detail, for both the cancer cell lines when only probe **PS** treated with already grown cancer cells in which it displays no fluorescence (MDA-MB-231) or very less (for A375). Besides, when both, probe **PS** (10 μM) and Hg^{2+} with different concentrations (5 & 10 μM) collectively treated with the grown MDA-MB-231 and A375 cells. It was found that probe **PS** strongly coordinating with the Hg^{2+} metal ion and it also exhibits strong fluorescence

while increasing the concentration of the Hg^{2+} metal ion. Therefore, based on these experimental results and observations, one can conclude that probe **PS** could be the best assortment to look at as a chemosensor for the recognition of intracellular Hg^{2+} metal ion.

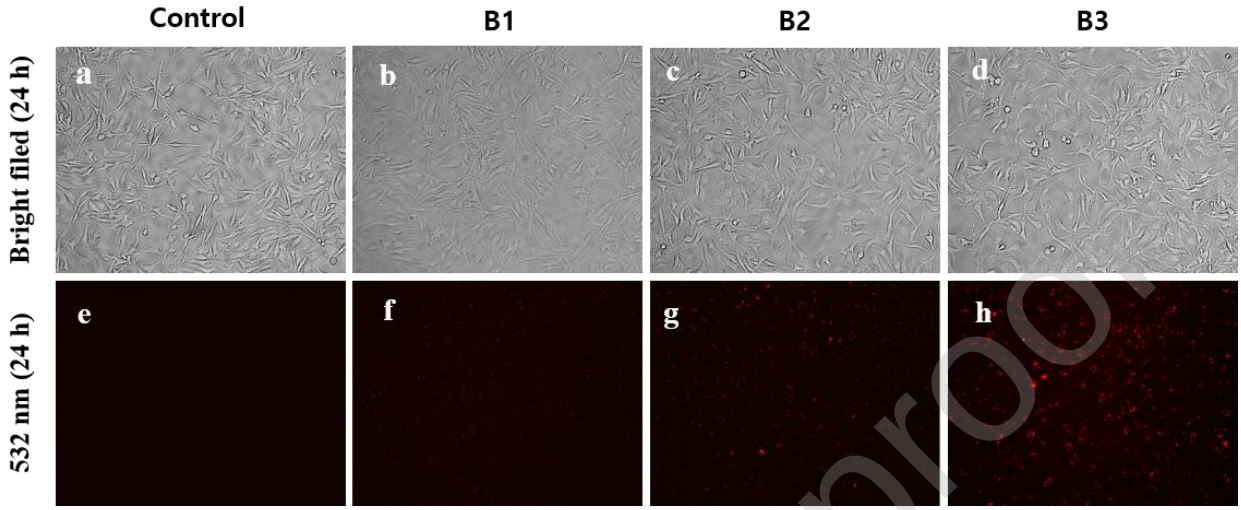

Fig. 9. Bright field transmission images of living MDA-MB-231 cells with control (a), Probe (PS) in DMSO (b), PS + 5 μM Hg^{2+} (c), and PS+ 10 μM Hg^{2+} (d) and fluorescence images of living MDA-MB-231 cells with control (e), Probe (PS) in DMSO (f), PS + 5 μM Hg^{2+} (g), and PS+ 10 μM Hg^{2+} (h) by exposing at 532 nm.

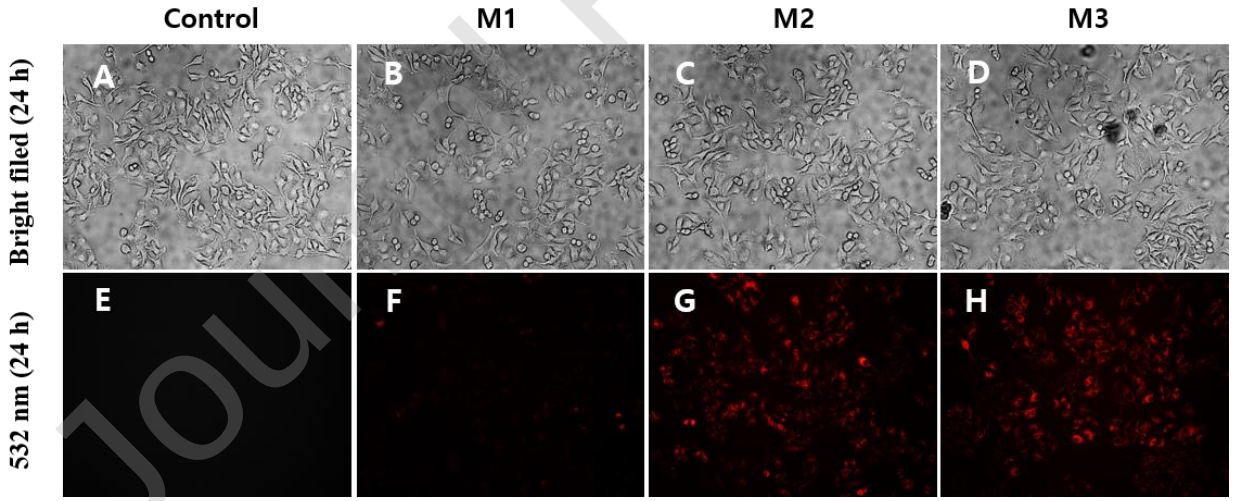

Fig. 10. Bright field transmission images of living A375 cells with controls (A), Probe (PS) in DMSO (B), PS + 5 μM Hg^{2+} (C), and PS+ 10 μM Hg^{2+} (D) and fluorescence images of living MDA-MB-231 cells with control (E), Probe (PS) in DMSO (F), PS + 5 μM Hg^{2+} (G), and PS+ 10 μM Hg^{2+} (H) by exposing at 532 nm.

3.4.2.2 Cytotoxicity

The cytotoxic impact of the probe **PS** in the presence or absence of the Hg^{2+} metal ion was investigated using two cancer cells, for instance, MDA-MB-231 and A375 respectively, by using MTT assay method [21, 27, 30]. Owing to its non-toxic nature to the cell surface, dimethyl sulfoxide (DMSO) was used as a solvent in an overall experiment. Furthermore, the Probe **PS** (10 μM), Hg^{2+} (10 μM) and different concentrations of the Hg^{2+} (5, & 10 μM) over probe PS (10 μM) were treated with both the cancer cells for 24 h. The cell viability measurements performed on both the cancer cells and presented in **Fig. 11 (1 & 2).** The non-toxic behavior of all the tested samples was in the vicinity with control. Delightfully, all the samples including probe **PS,** and the PS-Hg^{2+} complex were found to be non-toxic to the breast cancer cell MDA-MB-231 and human melanoma A375 cell. From the above findings, it can be inferred that probe **PS** and its complex with Hg^{2+} ion is non-toxic and could be useful for intracellular detection of the Hg^{2+} metal ion.

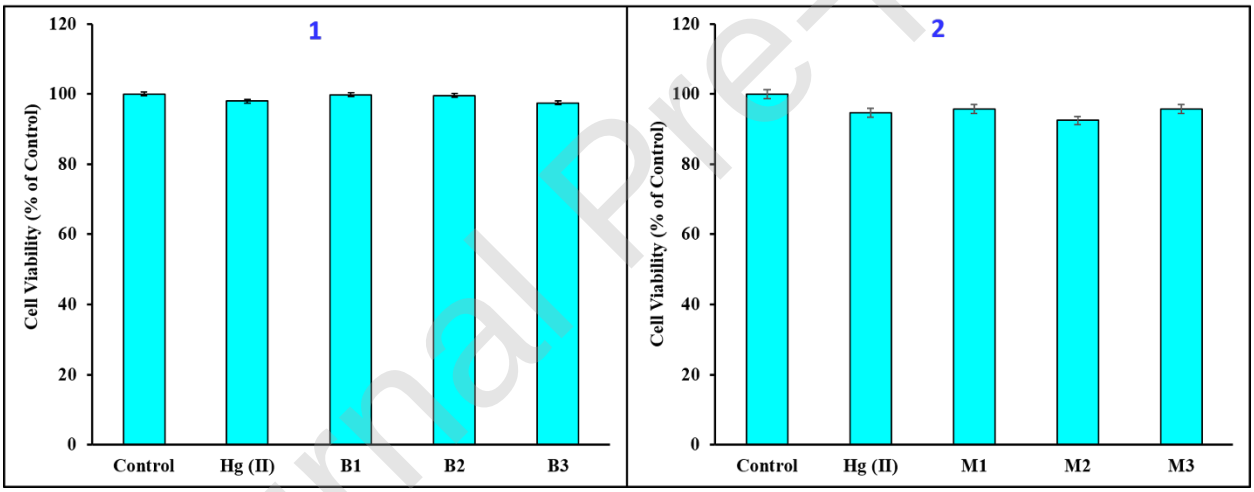

Fig. 11. Cell viability measurement using the MTT assay. (1) MDA-MB-231, cells were untreated (control)and cells treated with 10 μM Hg (II) metal ion, probe PS (B1), PS + 5 μM Hg^{2+} (B2) and PS + 10 μM Hg^{2+} (B3) for 24 h. (2) A-375, cells were untreated (control) and treated with10 μM Hg (II) metal ion, probe PS (M1), PS + 5 μM Hg^{2+} (M2) and PS + 10 μM Hg^{2+} (M3) for 24 h.

4. Conclusion:

In conclusion, we have designed an efficient fluorescent "off-on" chemosensor **PS** for the recognition of the Hg^{2+} in the mixed organic and aqueous phase. The probe **PS** displayed high

discerning and sensitive fluorescent enhancement towards Hg^{2+} metal ion, in which the transformation of the spirocyclic form (spirolactum) to open ring form was accomplished after the addition of the Hg^{2+}. Moreover, probe **PS** demonstrated chelation enhanced mechanism towards Hg^{2+} metal ion with 1:1 binding stoichiometry which was validated by Jobs plot and ^{1}H NMR titration experiment. The limit of detection (LOD) estimated for Hg^{2+} observed 3.0375×10^{-8} M (30.37 nM) utilizing the proposed approach and its superiority systematically explained and equated with other reported methods. The primary inspections in real water sample utilizing tap and drinking water signify that probe **PS** proves the selectivity in the identification of the Hg^{2+} metal ion even though in the existence of additional metal ions employing spike and recovery method, which draw attention to its prospective advantage in the field. Also, chemosensor **PS** was demonstrated to be an effective fluorescent "off-on" chemosensor for recognition of Hg^{2+} intracellularly using MDA-MB231 and A375 cancer cells. As a result, the low detection limit (LOD), utilization of water system in sensing assessment, useful applicability to ordinary water sample evaluation, and cell imaging and cytotoxicity study are the foremost gains of our research methodology.

CRediT AUTHOR STATEMENT

All persons who meet authorship criteria are listed as authors, and all authors certify that they have participated sufficiently in the work to take public responsibility for the content, including participation in the concept, design, analysis, writing, or revision of the manuscript. Furthermore, each author certifies that this material or similar material has not been and will not be submitted to or published in any other publication before its appearance in the **"Sensors & Actuators: B. Chemical".**

Authorship contributions:

Category 1 Conception and design of study: B. D. Vanjare, K. H. Lee;

acquisition of data: B. D. Vanjare, P.G. Mahajan, H. I. Ryoo, N.C. Dige, N. G. Choi, Y. Han, C. H. Kim;

analysis and/or interpretation of data: B. D. Vanjare, S. J. Kim, K. H. Lee;

Category 2 Drafting the manuscript: B. D. Vanjare, K. H. Lee;

revising the manuscript critically for important intellectual content: B. D. Vanjare, S. J. Kim, K.H. Lee;

Category 3 Approval of the version of the manuscript to be published (the names of all authors must be listed): B. D. Vanjare, P. G. Mahajan, H. I. Ryoo, N. C. Dige, N. G. Choi, Y. Han, S. J. Kim, C. H. Kim, K. H. Lee.

5. Acknowledgments

This research was supported by Basic Science Research Program through the National Research Foundation of Korea (NRF) funded by the Ministry of Education (NRF-2019R1I1A3A01059089).

Conflict of interest: Authors declares no conflict of interest.

6. References:

[1] Z.E. Chen, H. Zhang, Z. Iqbal, A new thiosemicarbazone fluorescent probe based on 9,9′-bianthracene for Hg^{2+} and Ag^{+}, Spectrochim. Acta - Part A Mol. Biomol. Spectrosc. 215 (2019) 34–40. https://doi.org/10.1016/j.saa.2019.02.036.

[2] D. Wu, A.C. Sedgwick, T. Gunnlaugsson, E.U. Akkaya, J. Yoon, T.D. James, Fluorescent chemosensors: the past, present and future, Chem. Soc. Rev. 46(23) (2017) 7105-7123. https://doi.org/ 10.1039/c7cs00240h

[3] A.E. Lee, M.R. Grace, A.G. Meyer, K.L. Tuck, Fluorescent Zn^{2+} chemosensors, functional in aqueous solution under environmentally relevant conditions, Tetrahedron Lett. 51 (2010) 1161–1165. https://doi.org/10.1016/j.tetlet.2009.12.069.

[4] J.H. Wang, Y.M. Liu, Z.M. Dong, J. Bin Chao, H. Wang, Y. Wang, S.M. Shuang, New colorimetric and fluorometric chemosensor for selective Hg^{2+} sensing in a near-perfect aqueous solution and bio-imaging, J. Hazard. Mater. 382 (2020) 121056. https://doi.org/10.1016/j.jhazmat.2019.121056.

[5] P.G. Mahajan, N.C. Dige, B.D. Vanjare, A.R. Phull, S.J. Kim, K.H. Lee, Gallotannin mediated silver colloidal nanoparticles as multifunctional nano platform: Rapid colorimetric and turn-on fluorescent sensor for Hg^{2+}, catalytic and In vitro anticancer activities, J. Lumin. 206 (2019). https://doi.org/10.1016/j.jlumin.2018.10.095.

[6] F. Ye, X.M. Liang, K.X. Xu, X.X. Pang, Q. Chai, Y. Fu, A novel dithiourea-appended naphthalimide "on-off" fluorescent probe for detecting Hg^{2+} and Ag^{+} and its application in

cell imaging, Talanta. 200 (2019) 494–502. https://doi.org/10.1016/j.talanta.2019.03.076.

[7] C. Zhang, H. Zhang, M. Li, Y. Zhou, G. Zhang, L. Shi, Q. Yao, S. Shuang, C. Dong, A turn-on reactive fluorescent probe for Hg^{2+} in 100% aqueous solution, Talanta. 197 (2019) 218–224. https://doi.org/10.1016/j.talanta.2019.01.016.

[8] H. Wang, X. Wang, M. Liang, G. Chen, R.M. Kong, L. Xia, F. Qu, A Boric Acid-Functionalized Lanthanide Metal-Organic Framework as a Fluorescence 'turn-on' Probe for Selective Monitoring of Hg^{2+} and CH_3Hg^+, Anal. Chem. 92 (2020) 3366–3372. https://doi.org/10.1021/acs.analchem.9b05410.

[9] L. Guo, Y. Song, K. Cai, L. Wang, "On-off" ratiometric fluorescent detection of Hg^{2+} based on N-doped carbon dots-rhodamine B@TAPT-DHTA-COF, Spectrochim. Acta - Part A Mol. Biomol. Spectrosc. 227 (2020) 117703. https://doi.org/10.1016/j.saa.2019.117703.

[10] X. Pang, J. Dong, L. Gao, L. Wang, S. Yu, J. Kong, L. Li, Dansyl-peptide dual-functional fluorescent chemosensor for Hg^{2+} and biothiols, Dye. Pigment. 173 (2020) 107888. https://doi.org/10.1016/j.dyepig.2019.107888.

[11] H. Zhang, J. You, J. Wang, X. Dong, R. Guan, D. Cao, Highly luminescent carbon dots as temperature sensors and "off-on" sensing of Hg^{2+} and biothiols, Dye. Pigment. 173 (2020) 107950. https://doi.org/10.1016/j.dyepig.2019.107950.

[12] Y. Gao, C. Zhang, S. Peng, H. Chen, A fluorescent and colorimetric probe enables simultaneous differential detection of Hg^{2+} and Cu^{2+} by two different mechanisms, Sensors Actuators, B Chem. 238 (2017) 455–461. https://doi.org/10.1016/j.snb.2016.07.076.

[13] S. Liu, L. Zhang, J. Gao, J. Zhou, Synthesis and analytical application of a novel fluorescent Hg^{2+} Probe 3′, 6′-bis(diethylamino)-2-((2,4-dimethoxybenzylidene)amino) spiro[isoindoline-1,9′-xanthene]-3-thione, J. Fluoresc. 23 (2013) 989–996. https://doi.org/10.1007/s10895-013-1225-7.

[14] L. Huang, Z. Yang, Z. Zhou, Y. Li, S. Tang, W. Xiao, M. Hu, C. Peng, Y. Chen, B. Gu, H. Li, A dual colorimetric and near-infrared fluorescent turn-on probe for Hg^{2+} detection and its applications, Dye. Pigment. 163 (2019) 118–125. https://doi.org/10.1016/j.dyepig.2018.11.047.

[15] L. Wang, J. Guo, X. Xiang, Y. Sang, J. Huang, Melamine-supported porous organic

polymers for efficient CO_2 capture and Hg^{2+} removal, Chem. Eng. J. 387 (2020). https://doi.org/10.1016/j.cej.2020.124070.

[16] Y. Wang, X. Hou, Z. Li, C. Liu, S. Hu, C. Li, Z. Xu, Y. Wang, A novel hemicyanine-based near-infrared fluorescent probe for Hg^{2+} ions detection and its application in living cells imaging, Dye. Pigment. 173 (2020) 107951. https://doi.org/10.1016/j.dyepig.2019.107951.

[17] Y. Wu, X. Wen, Z. Fan, An AIE active pyrene based fluorescent probe for selective sensing Hg^{2+} and imaging in live cells, Spectrochim. Acta - Part A Mol. Biomol. Spectrosc. 223 (2019) 117315. https://doi.org/10.1016/j.saa.2019.117315.

[18] L. Zong, Y. Xie, Q. Li, Z. Li, A new red fluorescent probe for Hg^{2+} based on naphthalene diimide and its application in living cells, reversibility on strip papers, Sensors Actuators, B Chem. 238 (2017) 735–743. https://doi.org/10.1016/j.snb.2016.07.052.

[19] Y. Ge, A. Liu, R. Ji, S. Shen, X. Cao, Detection of Hg^{2+} by a FRET ratiometric fluorescent probe based on a novel pyrido[1,2-a]benzimidazole-rhodamine system, Sensors Actuators, B Chem. 251 (2017) 410–415. https://doi.org/10.1016/j.snb.2017.05.097.

[20] J. Qiu, S. Jiang, B. Lin, H. Guo, F. Yang, An unusual AIE fluorescent sensor for sequentially detecting Co^{2+}-Hg^{2+}-Cu^{2+} based on diphenylacrylonitrile Schiff-base derivative, Dye. Pigment. 170 (2019). https://doi.org/10.1016/j.dyepig.2019.107590.

[21] B.D. Vanjare, P.G. Mahajan, N.C. Dige, A.R. Phull, S.J. Kim, K.H. Lee, Synthesis and Studies on Photophysical Properties of Rhodamine Derivatives for Bioimaging Applications, Bull. Korean Chem. Soc. (2019). https://doi.org/10.1002/bkcs.11733.

[22] X. Wang, T. Li, A novel "off-on" rhodamine-based colorimetric and fluorescent chemosensor based on hydrolysis driven by aqueous medium for the detection of Fe^{3+}, Spectrochim. Acta - Part A Mol. Biomol. Spectrosc. 229 (2020) 117951. https://doi.org/10.1016/j.saa.2019.117951.

[23] L.L. Yang, S.Y. Zou, Y.H. Fu, W. Li, X.P. Wen, P.Y. Wang, Z.C. Wang, G.P. Ouyang, Z. Li, S. Yang, Highly Selective and Sensitive Detection of Biogenic Defense Phytohormone Salicylic Acid in Living Cells and Plants Using a Novel and Viable Rhodamine-Functionalized Fluorescent Probe, J. Agric. Food Chem. 68 (2020) 4285–4291. https://doi.org/10.1021/acs.jafc.9b06771.

[24] B.D. Vanjare, P.G. Mahajan, N.C. Dige, H. Raza, M. Hassan, S.Y. Seo, K.H. Lee, Synthesis of novel xanthene based analogues: Their optical properties, jack bean urease inhibition and molecular modelling studies, Spectrochim. Acta - Part A Mol. Biomol. Spectrosc. 241 (2020) 118667. https://doi.org/10.1016/j.saa.2020.118667.

[25] a) Y. Wang, H. Ding, Z. Zhu, C. Fan, Y. Tu, G. Liu, S. Pu, Selective rhodamine–based probe for detecting Hg^{2+} and its application as test strips and cell staining, J. Photochem. Photobiol. A Chem. 390 (2020) 112302. https://doi.org/10.1016/j.jphotochem.2019.112302.

b) P.G. Mahajan, N.C. Dige, B.D. Vanjare, E. Kamaraj, S.Y. Seo, K.H. Lee, Nano molar level chromogenic and fluorogenic sensing of heavy metal ions using multi-responsive novel Schiff base as a dual mode chemosensor, J. Photochem. Photobiol. A Chem. 385 (2019) 112089. https://doi.org/10.1016/j.jphotochem.2019.112089.

[26] L. Yan, M. Yang, X. Leng, M. Zhang, Y. Long, B. Yang, A new dual-function fluorescent probe of Fe^{3+} for bioimaging and probe-Fe^{3+} complex for selective detection of CN−, Tetrahedron. 72 (2016) 4361–4367. https://doi.org/10.1016/j.tet.2016.05.082.

[27] P.G. Mahajan, J.S. Shin, N.C. Dige, B.D. Vanjare, Y. Han, N.G. Choi, S.J. Kim, S.Y. Seo, K.H. Lee, Chelation enhanced fluorescence of rhodamine based novel organic nanoparticles for selective detection of mercury ions in aqueous medium and intracellular cell imaging, J. Photochem. Photobiol. A Chem. 397 (2020) 112579. https://doi.org/10.1016/j.jphotochem.2020.112579.

[28] P.G. Mahajan, N.C. Dige, B.D. Vanjare, S.H. Eo, S.J. Kim, K.H. Lee, A nano sensor for sensitive and selective detection of Cu^{2+} based on fluorescein: Cell imaging and drinking water analysis, Spectrochim. Acta - Part A Mol. Biomol. Spectrosc. 216 (2019) 105–116. https://doi.org/10.1016/j.saa.2019.03.021.

[29] A. Roy, U. Shee, A. Mukherjee, S.K. Mandal, P. Roy, Rhodamine-Based Dual Chemosensor for Al^{3+} and Zn^{2+} Ions with Distinctly Separated Excitation and Emission Wavelengths, ACS Omega. 4 (2019) 6864–6875. https://doi.org/10.1021/acsomega.9b00475.

[30] P.G. Mahajan, N.C. Dige, B.D. Vanjare, Y. Han, S.J. Kim, S.K. Hong, K.H. Lee, Intracellular imaging of zinc ion in living cells by fluorescein based organic nanoparticles, Sensors Actuators, B Chem. 267 (2018) 119–128.

https://doi.org/10.1016/j.snb.2018.03.186.

[31] S.R. Liu, S.P. Wu, New water-soluble highly selective fluorescent chemosensor for Fe (III) ions and its application to living cell imaging, Sensors Actuators, B Chem. 171–172 (2012) 1110–1116. https://doi.org/10.1016/j.snb.2012.06.041.

[32] B. Das, A. Jana, A. Das Mahapatra, D. Chattopadhyay, A. Dhara, S. Mabhai, S. Dey, Fluorescein derived Schiff base as fluorimetric zinc (II) sensor via 'turn on' response and its application in live cell imaging, Spectrochim. Acta - Part A Mol. Biomol. Spectrosc. 212 (2019) 222–231. https://doi.org/10.1016/j.saa.2018.12.053.

[33] Y. Yu, L.R. Lin, K. Bin Yang, X. Zhong, R. Bin Huang, L.S. Zheng, P-Dimethylaminobenzaldehyde thiosemicarbazone: A simple novel selective and sensitive fluorescent sensor for mercury(II) in aqueous solution, Talanta. 69 (2006) 103–106. https://doi.org/10.1016/j.talanta.2005.09.015.

[34] P.G. Mahajan, N.C. Dige, B.D. Vanjare, A.R. Phull, S.J. Kim, K.H. Lee, Gallotannin mediated silver colloidal nanoparticles as multifunctional nano platform: Rapid colorimetric and turn-on fluorescent sensor for Hg^{2+}, catalytic and In vitro anticancer activities, J. Lumin. 206 (2019) 624–633. https://doi.org/10.1016/j.jlumin.2018.10.095.

[35] Y.C. Hsieh, J.L. Chir, H.H. Wu, P.S. Chang, A.T. Wu, A sugar-aza-crown ether-based fluorescent sensor for Hg^{2+} and Cu^{2+}, Carbohydr. Res. 344 (2009) 2236–2239. https://doi.org/10.1016/j.carres.2009.08.027.

[36] J.S. Do, K.H. Lin, R. Ohara, Preparation of urease/nano-structured polyaniline-Nafion®/Au/Al_2O_3 electrode for inhibitive detection of mercury ion, J. Taiwan Inst. Chem. Eng. 42 (2011) 662–668. https://doi.org/10.1016/j.jtice.2010.11.007.

[37] T.K. Vel Krawczyk, M. Moszczyńska, M. Trojanowicz, Inhibitive determination of mercury and other metal ions by potentiometric urea biosensor, Biosens. Bioelectron. 15 (2000) 681–691. https://doi.org/10.1016/S0956-5663(00)00085-3.

[38] E. Coronado, J.R. Galán-Mascarós, C. Martí-Gastaldo, E. Palomares, J.R. Durrant, R. Villar, M. Gratzel, M.K. Nazeeruddin, Reversible colorimetric probes for mercury sensing, J. Am. Chem. Soc. 127 (2005) 12351–12356. https://doi.org/10.1021/ja0517724.

[39] M.L. Firdaus, I. Fitriani, S. Wyantuti, Y.W. Hartati, R. Khaydarov, J.A. Mcalister, H. Obata, T. Gamo, Colorimetric detection of mercury(II) ion in aqueous solution using silver nanoparticles, Anal. Sci. 33 (2017) 831–837. https://doi.org/10.2116/analsci.33.831.

[40] H. El Kaoutit, P. Estévez, F.C. García, F. Serna, J.M. García, Sub-ppm quantification of Hg(II) in aqueous media using both the naked eye and digital information from pictures of a colorimetric sensory polymer membrane taken with the digital camera of a conventional mobile phone, Anal. Methods. 5 (2013) 54–58. https://doi.org/10.1039/c2ay26307f.

[41] Y. Yang, Z. Wang, M. Yang, M. Guo, Z. Wu, G. Shen, Inhibitive determination of mercury ion using a renewable urea biosensor based on self-assembled gold nanoparticles, Sensors Actuators, B Chem. 114 (2006) 1–8. https://doi.org/10.1016/j.snb.2005.04.005.

[42] G.H. Chen, W.Y. Chen, Y.C. Yen, C.W. Wang, H.T. Chang, C.F. Chen, Detection of mercury (II) ions using colorimetric gold nanoparticles on paper-based analytical devices, Anal. Chem. 86 (2014) 6843–6849. https://doi.org/10.1021/ac5008688.

[43] N. Zohora, D. Kumar, M. Yazdani, V.M. Rotello, R. Ramanathan, V. Bansal, Rapid colorimetric detection of mercury using biosynthesized gold nanoparticles, Colloids Surfaces A Physicochem. Eng. Asp. 532 (2017) 451–457. https://doi.org/10.1016/j.colsurfa.2017.04.036.

[44] A. Samphao, H. Rerkchai, J. Jitcharoen, D. Nacapricha, K. Kalcher, Indirect determination of mercury by inhibition of glucose oxidase immobilized on a carbon paste electrode, Int. J. Electrochem. Sci. 7 (2012) 1001–1010.

[45] N.R. Devi, M. Sasidharan, A.K. Sundramoorthy, Gold Nanoparticles-Thiol-Functionalized Reduced Graphene Oxide Coated Electrochemical Sensor System for Selective Detection of Mercury Ion, J. Electrochem. Soc. 165 (2018) B3046–B3053. https://doi.org/10.1149/2.0081808jes.

[46] O. García-Beltrán, A. Rodríguez, A. Trujillo, A. Cañete, P. Aguirre, S. Gallego-Quintero, M.T. Nuñez, M.E. Aliaga, Synthesis and characterization of a novel fluorescent and colorimetric probe for the detection of mercury (II) even in the presence of relevant biothiols, Tetrahedron Lett. 56 (2015) 5761–5766. https://doi.org/10.1016/j.tetlet.2015.09.001.

[47] S. Chen, W. Wang, M. Yan, Q. Tu, S.W. Chen, T. Li, M. Sen Yuan, J. Wang, 2-Hydroxy benzothiazole modified rhodol: aggregation-induced emission and dual-channel fluorescence sensing of Hg^{2+} and Ag^{+} ions, Sensors Actuators, B Chem. 255 (2018) 2086–2094. https://doi.org/10.1016/j.snb.2017.09.008.

[48] T.B. Wei, G.Y. Gao, W.J. Qu, B.B. Shi, Q. Lin, H. Yao, Y.M. Zhang, Selective

fluorescent sensor for mercury(II) ion based on an easy to prepare double naphthalene Schiff base, Sensors Actuators, B Chem. 199 (2014) 142–147. https://doi.org/10.1016/j.snb.2014.03.084.

[49] R. Zhang, W. Chen, Nitrogen-doped carbon quantum dots: Facile synthesis and application as a 'turn-off' fluorescent probe for detection of Hg^{2+} ions, Biosens. Bioelectron. 55 (2013) 83–90. https://doi.org/10.1016/j.bios.2013.11.074.

[50] Y. Zou, M. Wan, G. Sang, M. Ye, Y. Li, An alternative copolymer of carbazole and thieno[3,4b]-pyrazine: Synthesis and mercury detection, Adv. Funct. Mater. 18 (2008) 2724–2732. https://doi.org/10.1002/adfm.200800567.

[51] M.H. Yang, P. Thirupathi, K.H. Lee, Selective and sensitive ratiometric detection of Hg(II) ions using a simple amino acid based sensor, Org. Lett. 13 (2011) 5028–5031. https://doi.org/10.1021/ol201683t.

[52] H.S. So, B.A. Rao, J. Hwang, K. Yesudas, Y.A. Son, Synthesis of novel squaraine-bis(rhodamine-6G): A fluorescent chemosensor for the selective detection of Hg^{2+}, Sensors Actuators, B Chem. 202 (2014) 779–787. https://doi.org/10.1016/j.snb.2014.06.013.

[53] S.Y. Lin, H.J. Zhu, W.J. Xu, G.M. Wang, N.Y. Fu, A squaraine based fluorescent probe for mercury ion via coordination induced deaggregation signaling, Chinese Chem. Lett. 25 (2014) 1291–1295. https://doi.org/10.1016/j.cclet.2014.04.027.

[54] a) V. Bhalla, R. Tejpal, M. Kumar, Rhodamine appended terphenyl: A reversible 'off-on' fluorescent chemosensor for mercury ions, Sensors Actuators, B Chem. 151 (2010) 180–185. https://doi.org/10.1016/j.snb.2010.09.024.

b) B. Yuan, D.X. Wang, L.N. Zhu, Y.L. Lan, M. Cheng, L.M. Zhang, J.Q. Chu, X.Z. Li, D.M. Kong, Dinuclear HgII tetracarbene complex-triggered aggregation-induced emission for rapid and selective sensing of Hg2+ and organomercury species, Chem. Sci. 10 (2019) 4220–4226. https://doi.org/10.1039/c8sc05714a.

c) A. Chatterjee, M. Banerjee, D.G. Khandare, R.U. Gawas, S.C. Mascarenhas, A. Ganguly, R. Gupta, H. Joshi, Aggregation-Induced Emission-Based Chemodosimeter Approach for Selective Sensing and Imaging of Hg(II) and Methylmercury Species, Anal. Chem. 89 (2017) 12698–12704. https://doi.org/10.1021/acs.analchem.7b02663.

[55] B.D. Vanjare, P.G. Mahajan, S.-K. Hong, K.H. Lee, Discriminating Chemosensor for

Detection of Fe^{3+} in Aqueous Media by Fluorescence Quenching Methodology, Bull. Korean Chem. Soc. 39 (2018). https://doi.org/10.1002/bkcs.11442.

[56] S.K. Patil, D. Das, A novel rhodamine-based optical probe for mercury(II) ion in aqueous medium: A nanomolar detection, wide pH range and real water sample application, Spectrochim. Acta - Part A Mol. Biomol. Spectrosc. 225 (2020) 117504. https://doi.org/10.1016/j.saa.2019.117504.

[57] D. Wu, W. Huang, Z. Lin, C. Duan, C. He, S. Wu, D. Wang, Highly sensitive multiresponsive chemosensor for selective detection of Hg^{2+} in natural water and different monitoring environments, Inorg. Chem. 47 (2008) 7190–7201. https://doi.org/10.1021/ic8004344.

[58] M.J. Culzoni, A. Muñoz De La Peña, A. MacHuca, H.C. Goicoechea, R. Babiano, Rhodamine and BODIPY chemodosimeters and chemosensors for the detection of Hg^{2+}, based on fluorescence enhancement effects, Anal. Methods. 5 (2013) 30–49. https://doi.org/10.1039/c2ay25769f.

[59] S. Saha, P. Mahato, U. Reddy G, E. Suresh, A. Chakrabarty, M. Baidya, S.K. Ghosh, A. Das, Recognition of Hg^{2+} and Cr^{3+} in physiological conditions by a rhodamine derivative and its application as a reagent for cell-imaging studies, Inorg. Chem. 51 (2012) 336–345. https://doi.org/10.1021/ic2017243.

[60] T. Du, J. Wang, T. Zhang, L. Zhang, C. Yang, T. Yue, J. Sun, T. Li, M. Zhou, J. Wang, An Integrating Platform of Ratiometric Fluorescent Adsorbent for Unconventional Real-Time Removing and Monitoring of Copper Ions, ACS Appl. Mater. Interfaces. 12 (2020) 13189–13199. https://doi.org/10.1021/acsami.9b23098.

[61] X. Liu, L. Huang, Y. Wang, J. Sun, T. Yue, W. Zhang, J. Wang, One-pot bottom-up fabrication of a 2D/2D heterojuncted nanozyme towards optimized peroxidase-like activity for sulfide ions sensing, Sensors Actuators, B Chem. 306 (2020) 127565. https://doi.org/10.1016/j.snb.2019.127565.

Biographies

Balasaheb D. Vanjare: Received his M. Sc (Organic Chemistry) from the Fergusson College, University of Pune, Pune, Maharashtra, India. Currently he is pursuing his Ph.D. degree in research group of Prof. Ki Hwan Lee, Kongju National University, Gongju, South Korea. His

research interests include synthesis, characterization of novel organic compounds and utilization them in chemo-sensing, cell imaging, biological activities, and analysis of environmental samples.

Prasad G. Mahajan: received his Ph.D. Degree in Chemistry from Shivaji University, Kolhapur, Maharashtra, India. He worked as a Post-Doctoral Research Associate in Prof. Ki Hwan Lee's research group at Kongju National University, Gongju, South Korea. His current research activities focus on the synthesis of organic compounds and metal nanoparticles for the utility as probe in the field of photodynamic therapy, colorimetric and fluorometric sensors, cell imaging, biological activities, and analysis of environmental samples.

Hyang-Im Ryoo: Received her Ph.D. Degree in chemical engineering and applied chemistry from the Chungnam National University, Yuseong-gu, Daejeon, South Korea. Currently she is working in as a Post-Doctoral Research Associate in Prof. Ki Hwan Lee's research group at Kongju National University, Gongju, South Korea. Her research work includes the Synthesis of the fluorescent organic compounds and its application as a fluorescent chemosensor for the detection of the heavy metal ions.

Nilam C. Dige: received her Ph.D. Degree in Chemistry from Shivaji University, Kolhapur, Maharashtra, India. She worked as a Post-Doctoral Research Associate in Prof. Sung-Yum Seo research group at Kongju National University, Gongju, South Korea. Her current research activities encompass the synthesis of variety of heterocyclic compounds using multicomponent reaction approach and utilization them in biological studies.

Nam Gyu Choi: Currently working as Master student in research group of Prof. Ki Hwan Lee, Kongju National University, Gongju, South Korea. His research interests include the synthesis of the organic compounds and their application as a fluorescent chemosensor.

Yohan Han is currently working as Post-Doctoral Research Associate in Prof. Song Ja Kim's research group at Kongju National University, Gongju, South Korea. His research area is cell signaling in chondrocytes and cancer cells.

Song Ja Kim is currently working as a Professor in Department of Biological Sciences, Kongju National University, Gongju, South Korea. Her research mainly focuses on molecular cell biology, biotechnology, cell imaging and cell signaling in chondro-cytes and cancer cells.

Chong-Hyeak Kim is a research fellow in the chemical analysis center at Korea Research Institute of Chemical Technology (KRICT). He received his Ph.D. from the University of Tokyo in the department of chemistry in 1996 under the supervision of Prof. Toschitake Iwamoto. And he worked as a postdoctoral researcher in Prof. David. A. Atwood' group at the University of Kentucky (2000–2001). His research interests include 3-D structure analysis using X-ray crystallography, technical education, and training on chemical analysis.

Ki Hwan Lee is currently a Professor of Physical Chemistry in the Department of Chemistry at Kongju National University, Gongju, South Korea. The design, synthesis, and application of varieties of photoactive heterocyclic organic compounds in biological and environmental fields are the current research interests of Prof. Lee.